PAPER

# An Overview of Autonomous Underwater Vehicle Research and Testbed at PeRL

AUTHORS
Hunter C. Brown
Ayoung Kim
Ryan M. Eustice
University of Michigan

ABSTRACT

This article provides a general overview of the autonomous underwater vehicle (AUV) research thrusts being pursued within the Perceptual Robotics Laboratory (PeRL) at the University of Michigan. Founded in 2007, PeRL's research centers on improving AUV autonomy via algorithmic advancements in environmentally based perceptual feedback for real-time mapping, navigation, and control. Our three major research areas are (1) real-time visual simultaneous localization and mapping (SLAM), (2) cooperative multi-vehicle navigation, and (3) perception-driven control. Pursuant to these research objectives, PeRL has developed a new multi-AUV SLAM testbed based upon a modified Ocean-Server Iver2 AUV platform. PeRL upgraded the vehicles with additional navigation and perceptual sensors for underwater SLAM research. In this article, we detail our testbed development, provide an overview of our major research thrusts, and put into context how our modified AUV testbed enables experimental real-world validation of these algorithms.
Keywords: AUVs, SLAM, navigation, mapping, testbed

## Introduction

The Perceptual Robotics Laboratory (PeRL) at the University of Michigan (UMich) is actively involved in three major research efforts: real-time vision-based simultaneous localization and mapping (SLAM), heterogeneous multi-vehicle cooperative navigation, and perception-driven control. To test and experimentally validate these algorithms, we have developed a new multi-autonomous underwater vehicle (AUV) testbed based upon a modified Ocean-Server Iver2 commercial AUV platform. This new AUV testbed provides a simple man-portable platform for real-world experimental validation and serves as a dedicated engineering testbed for proof-of-concept algorithmic implementations. In this article, we report on our developments in this area and provide an overview of this new experimental facility (Figure 1).

## Overview of Underwater Navigation

One of the major limitations in the field of underwater robotics is the lack of radio-frequency transmission modes. The opacity of water to electromagnetic waves precludes the use of the global positioning system (GPS) as well as high-speed underwater radio communication (Stewart, 1991). Hence, communication and navigation underwater must rely upon other means. Kinsey et al. (2006) provided an overview of the current state-of-the-art in underwater vehicle navigation, of which we briefly summarize here.

### *Conventional Underwater Navigation Systems*

Two broad categories of underwater navigation methods exist for localizing vehicles and instruments: absolute positioning and relative dead-reckoning. The traditional long-baseline (LBL) method of underwater

**FIGURE 1**

PeRL's multi-AUV testbed is based upon a modified Ocean-Server Iver2 AUV platform. Shown in the foreground is a modified vehicle displaying a new nose cone designed and fabricated by PeRL. For comparison, a stock vehicle displaying the original nose cone is shown in the background.

positioning estimates absolute position by measuring time-of-flight ranges to fixed beacons (Hunt et al., 1974; Milne, 1983). The precision of this estimate is bounded, and the accuracy is determined by system biases. The range of this solution is limited to a few kilometers in the best acoustic conditions, and the positioning resolution is on the order of 1 m. The slow update rate of LBL is constrained by the acoustic travel times—typically updating every few seconds. In contrast to slow, coarse, but absolute LBL positioning, a Doppler velocity log (DVL) or inertial navigation system (INS) instead estimates the distance traveled to infer position. Dead-reckoning is fast (~10 Hz) and delivers fine resolution (~1 cm), but the precision of this relative measurement is unbounded, growing monotonically with time. This makes it difficult to return to a known location or to relate measurements globally to one another.

### *Underwater SLAM*

Over the past decade, a significant research effort within the terrestrial mobile robotics community has been to develop environmentally based navigation algorithms that eliminate the need for additional infrastructure and bound position error growth to the size of the environment—a key prerequisite for truly autonomous navigation. The goal of this work has been to exploit the perceptual sensing capabilities of robots to correct for accumulated odometric error by localizing the robot with respect to landmarks in the environment (Bailey and Durrant-Whyte, 2006; Durrant-Whyte and Bailey, 2006).

One of the major challenges of the SLAM problem is (1) defining fixed features from raw sensor data and (2) establishing measurement to feature correspondence [i.e., the problem of data association (Neira and Tardos, 2001)]. Both of these tasks can be nontrivial—especially in an unstructured underwater environment. In man-made environments, typically composed of planes, lines, and corners primitives, point features can be more easily defined; however, complex underwater environments pose a more challenging task for feature extraction and matching.

One approach to curbing the challenges of defining fixed features from raw sensor data is to seed the environment with artificial landmarks that are easily recognizable. For example, one practical application of a range-only underwater SLAM has been to localize an AUV in an acoustic-beacon network that has *a priori* unknown geometry (Newman and Leonard, 2003; Olson et al., 2006). In this scenario, the beacon geometry is learned online by the SLAM algorithm, eliminating the need to conduct an initial survey calibration of the acoustic-beacon network by a surface ship. Moreover, this paradigm can easily be extended to a scenario where the AUV self-deploys the acoustic beacons *in situ* over the survey site.

More recently, progress has been made in applying SLAM in an *a priori* unknown underwater environment without the aid of artificial landmarks. In particular, one SLAM methodology that has seen recent success in the benthic realm is to apply a pose-graph scan-matching approach (Fleischer, 2000; Eustice et al., 2006a). Pose-graph SLAM approaches do not require an explicit representation of features and instead use a data-driven approach based upon extracting relative-pose constraints from raw sensor data. The main idea behind this methodology is that registering overlapping perceptual data, for example, optical imagery as reported in by Eustice et al. (2006a, 2006b) or sonar bathymetry as reported by Roman and Singh (2005), introduces spatial drift-free edge constraints into the pose-graph. These spatial constraints effectively allow the robot to close-the-loop when revisiting a previously visited place, thereby resetting any accumulated dead-reckoning error.

## Overview of PeRL's Research Thrusts

PeRL's three major research areas are (1) real-time visual SLAM, (2) cooperative multi-vehicle navigation, and (3) perception-driven control. In this section, we provide an overview of our laboratory's research thrusts as they pertain to AUV algorithms.

### *Real-Time Visual SLAM*

The first of the three PeRL research domains, real-time vision-based SLAM algorithms, has direct application to areas such as autonomous underwater ship-hull inspection (Eustice, 2008; Kim and Eustice, 2009) and deep-sea archaeological missions (Ballard, 2008; Foley et al., 2009).

Present day means for ship-hull and port security inspection require either putting divers in the water or piloting a remotely operated vehicle (ROV) over the area of interest—both of these methods are manpower intensive and generally cannot quantitatively guarantee 100% survey coverage. Automating this task, however, is challenging and compounded by the fact that areas around ships in berth are severely confined, cluttered, and complex sensing environments (e.g., acoustically, optically, magnetically). Current tethered robotic inspection systems present issues of snagging, maneuver degradation, and tether management, all of which make maneuvering around the ship at the pier difficult. Moreover, current robotic inspection methods require human in-the-loop intervention for both sensory interpretation and control (e.g., ROV piloting). Navigation feedback in these scenarios is typically performed using acoustic transponder time-of-flight ranging (Smith and Kronen, 1997). This necessitates the setup and calibration of the acoustic-beacon infrastructure, and therefore vitiates our ability to rapidly and repeatedly inspect multiple underwater structures.

Similarly, deep-sea archaeology also requires high-performance navigation (Ballard, 2008; Foley et al., 2009). Optical imagery, bathymetric sonar, and environmental measurements are all products of interest to the archeologist. The data may be collected over multiple missions or even multiple field seasons, and it is the precision of the navigation that makes it possible to transform these measurements into co-registered maps.

To combat the aforementioned navigation limitations (i.e., infrastructure-based and unbounded error growth), PeRL has been developing a camera-based navigation system that uses vehicle-collected imagery of the hull (port/hull inspection) or seafloor (underwater archeology) to extract measurements of vehicle motion. These camera-derived spatial measurements are fused with the onboard dead-reckoned data to produce a bounded-error navigation estimate (Figure 2).

In essence, the AUV builds a digital map of the seafloor or hull by registering overlapping digital-still images (both along-track and cross-track imagery). Images that are successfully registered produce a relative measurement of the vehicle's attitude (heading, pitch, and roll) and translational (x, y, z) displacement. When fused with the onboard navigation data from a bottom-lock DVL, the result is a navigation system whose error is commensurate or much better than LBL but which is infrastructure free. The significant advantage of this navigation paradigm is that it is *in situ*. For archeological surveys, this means that the AUV can be more easily deployed for exploratory surveys to investigate target shipwreck sites—without having to invest significant ship time in deploying a beacon network to obtain precision navigation; and for hull inspection surveys, no additional acoustic-beacon infrastructure is required for precise global localization along the hull. In layman's terms, these algorithms allow the AUV to navigate much like a human does by visually navigating with respect to the seafloor environment.

A useful and important by-product of this navigation methodology is that the overlapping registered imagery can be used to construct an optically derived bathymetry map (Figure 3). This map can be used to construct a quantitatively accurate three-dimensional (3-D) photomosaic by back-projecting the imagery over the optical bathymetry map. Figure 3 displays the result of applying this technology to the fourth-century B.C. Chios classical ancient shipwreck site (Foley et al., 2009). In particular, Figure 3a shows the optically derived bathymetry map for a 15 m by 45 m swath centered overtop

**FIGURE 2**

The foundation of visually augmented navigation (Eustice et al., 2008) is the fusion of "zero-drift" camera measurements with dead-reckoned vehicle navigation data to produce a bounded error position estimate. These constraints are fused with onboard navigation sensor data in a view-based stochastic map framework; the model is composed of a pose-graph where the nodes correspond to historical robot poses and the edges represent either navigation or camera constraints.

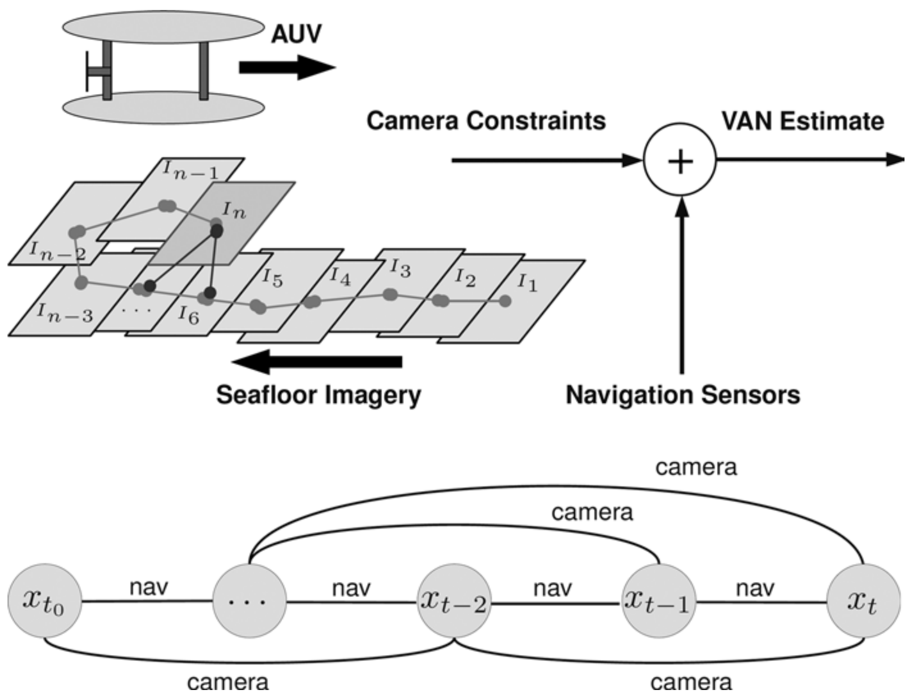

**FIGURE 3**

A by-product of camera-based AUV navigation is the ability to produce an optically derived bathymetry. VAN-derived bathymetric maps from the Chios 2005 shipwreck survey are depicted (Foley et al., 2009). (a) Triangulated 3-D point cloud from registered imagery. The point cloud is gridded to 5 cm to produce an optically derived bathymetry map. (b) A quantitatively correct 3-D mosaic is generated by back-projecting the imagery onto the optical bathymetry map. The gray areas correspond to regions of no image overlap. (c) A zoomed overhead view shows detail of the amphorae pile in the center mound of the 3-D photomosaic.

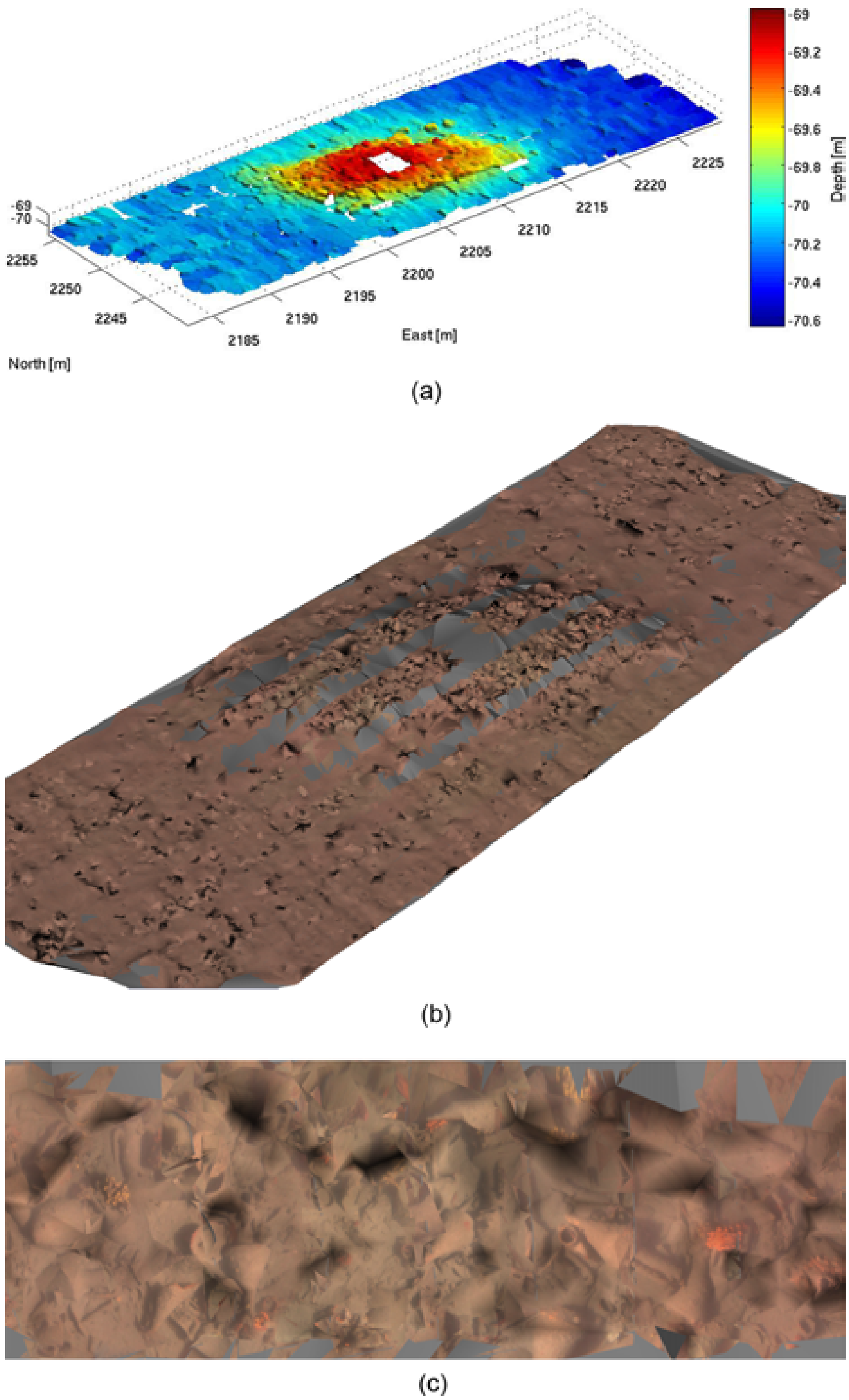


the wreck site. The optical bathymetry is generated from a 3-D triangulated point cloud derived from pixel correspondences. In Figure 3b, we display a quantitatively accurate 3-D photomosaic obtained by back-projecting the imagery onto the gridded surface. It should be emphasized that this result is fully automatic and metrically quantitative, in other words, measurements of object size and geometric relationships can be derived. Although this technology is still very much in the active research stage, its current and future value for *in situ*, rapid, quantitative documentation of marine archeological wreck sites or ship-hull inspection cannot be overstated.

### *Cooperative Navigation*

In addition to real-time visual SLAM, PeRL is working toward cooperative multi-vehicle missions for large-area survey. Multi-vehicle cooperative navigation offers promise of efficient exploration by groups of mobile robots working together to pool their mapping capability. Most prior research in the SLAM community has focused on the case of single-agent mapping and exploration. Although these techniques can often be extended to a centralized multi-agent framework (Walter and Leonard, 2004) (provided that there are no communication bandwidth restrictions), the extension of single-agent techniques to a decentralized multi-vehicle SLAM framework is often neither obvious nor appropriate. Much of the previous research in the area of distributed multi-vehicle SLAM has focused primarily on terrestrial (i.e., land and aerial) applications (Williams et al., 2002; Ridley et al., 2002; Rekleitis et al., 2003; Bourgault et al., 2004; Ong et al., 2006; Partan et al., 2006). There, high-bandwidth radio communication is possible; however, underwater communication bandwidth is distinctly limited from that on land (Partan et al., 2006).

It requires on the order of 100 times more power to transmit than it does to receive underwater, which makes acoustic transmission and reception asymmetrical for medium access schemes (Partan et al., 2006). Half duplex time division multiple access networks are usual, with typical acoustic-modem data rates ranging from 5 kbits/s at a range of 2 km (considered a high rate) to as little as 80 bits/s (a low rate). The low acoustic data rates are not simply a limitation of current technology—the theoretical performance limit for underwater acoustic communications is 40 km kbps (e.g., a max theoretical data rate of 20 kbps at a range of 2 km) (Partan et al., 2006). Therefore, any type of multi-vehicle SLAM framework must adhere to the physical bandwidth limitations of the underwater domain.

In a previous work, Eustice et al. (2006c, 2007) developed a synchronous clock acoustic-modem-based navigation system capable of supporting multi-vehicle ranging. The system consisted of a Woods Hole Oceanographic Institution (WHOI) Micro-Modem (Freitag et al., 2005a, 2005b) (an underwater acoustic modem developed by WHOI) and a low-power stable clock board. This system can be used as a synchronous-transmission communication/navigation system wherein data packets encode time of origin information as well as local ephemeris data (e.g., x, y, z positional data and error metric). This allows for the direct measurement of inter-vehicle one-way travel time (OWTT) time-of-flight ranging. The advantage of a OWTT ranging methodology is that all passively receiving nodes within listening range are able to decode and measure the inter-vehicle range to the broadcasting node.

PeRL is currently investigating probabilistic fusion methods for a OWTT cooperative navigation multi-vehicle framework that scales across a distributed network of nodes in a non-fully connected network topology. The proposed acoustic-modem navigation framework will exploit inter-vehicle OWTT ranging to supplement perceptual SLAM localization thereby reducing the need for state communication. The goal is to distribute state estimation between the vehicles in a coordinated fashion, allowing navigation impoverished vehicles (e.g., no INS or DVL) to share from positional accuracies of better equipped vehicles (e.g., those with DVL bottom-lock, or VAN-navigated vehicles near the seafloor).

Figure 4 depicts preliminary results reported by Eustice et al. (2007), demonstrating the OWTT proof of concept. Here, a GPS-equipped surface ship navigationally aided a submerged AUV by broadcasting the ship GPS position to the network while the AUV measured its range to the ship via the OWTTs.

### *Perception-Driven Control*

Another research focus is in the domain of perception-driven control. Algorithms are under development to enable a vehicle to respond to the environment by autonomously selecting alternative search patterns based upon perceived feature distributions in the environment. This creates improvements in survey efficiency by limiting the duration in benign feature-poor areas and instead spends more bottom-time over actual targets. A seafloor survey vehicle, for example, may drive into an area devoid of features during a mission. Instead of continuing to search the featureless space, where there is little return on investment from a visual navigation system, the vehicle would return to a previously known feature rich area and begin searching in another direction. PeRL is currently working on algorithms to

**FIGURE 4**

Preliminary OWTT results as reported by Eustice et al. (2007) for a two-node network consisting of an AUV and a surface ship. (left) The raw dead-reckoned AUV trajectory is shown in blue, GPS-derived ship position in cyan, OWTT fused AUV trajectory in red, and the LBL measured AUV position in green, which serves as an independent ground-truth. (right) Zoomed view of the AUV trajectory. (Color versions of figures available online at: http://www.ingentaconnect.com/content/mts/mtsj/2009/00000043/00000002.)

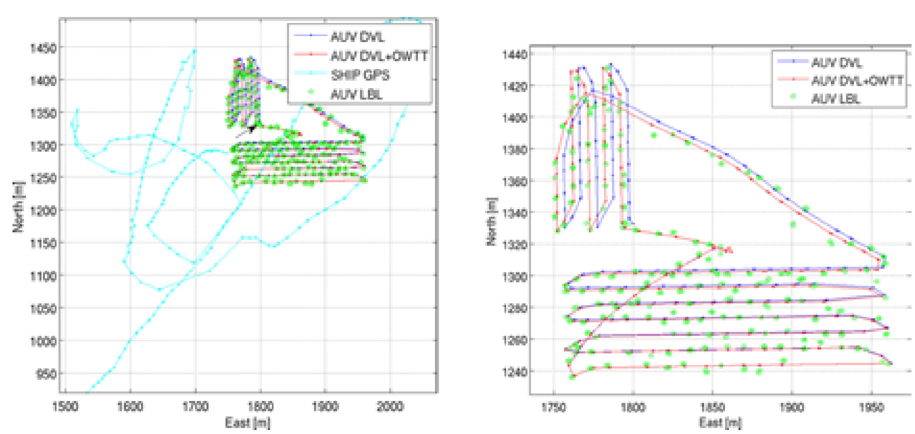

assist in the decision making process of when to revisit known landmarks versus continuing new exploration. For example, Figure 5 depicts imagery from a hull inspection survey of a decommissioned aircraft carrier (Kim and Eustice, 2009). At the one extreme, we see that some areas of the hull are very texture-rich (heavily biofouled), whereas other areas are nearly feature-less (no distinguishing features such as weld seams, rivets, port opening, etc). In this type of environment, it makes no sense to incorporate imagery from the featureless region into the visual SLAM map because the image registration algorithm will fail to localize the vehicle because of a lack of visual features. Instead, by coupling the visual navigation feedback into the trajectory planning and control, the AUV can more intelligently adapt its survey and map-building strategy so as to only return to feature-rich areas of the hull when it accrues too much pose uncertainty. By jointly considering along-hull pose uncertainty, map feature content, and energy expenditure accrued during AUV transit, we can frame the online path planning problem as a multi-objective optimization problem that seeks to find an optimal trajectory with respect to the possibly divergent criteria of exploration versus localization.

## Overview of PeRL's AUV Testbed

To pursue PeRL's three research thrust areas, two commercial Ocean-Server Iver2 AUV systems were purchased and modified to serve as a real-world testbed platform for SLAM research at UMich. Although several other vehicle platforms currently include stereo-vision systems and DVL sensors, the Iver2 (Figure 6) was

**FIGURE 5**

Depiction of the multi-objective constraints at play in perception-driven control.

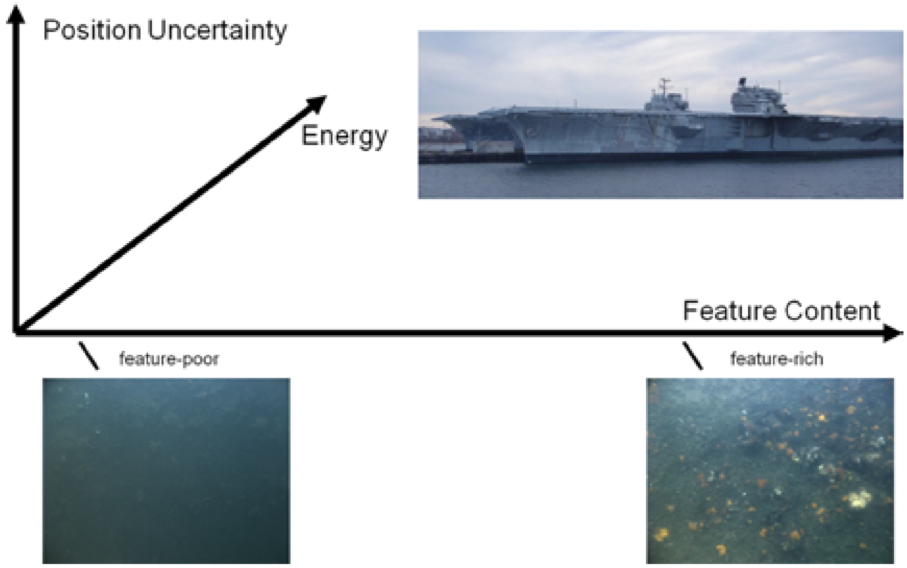


**FIGURE 6**

PeRL's modified Ocean-Server Iver2: external and internal view.

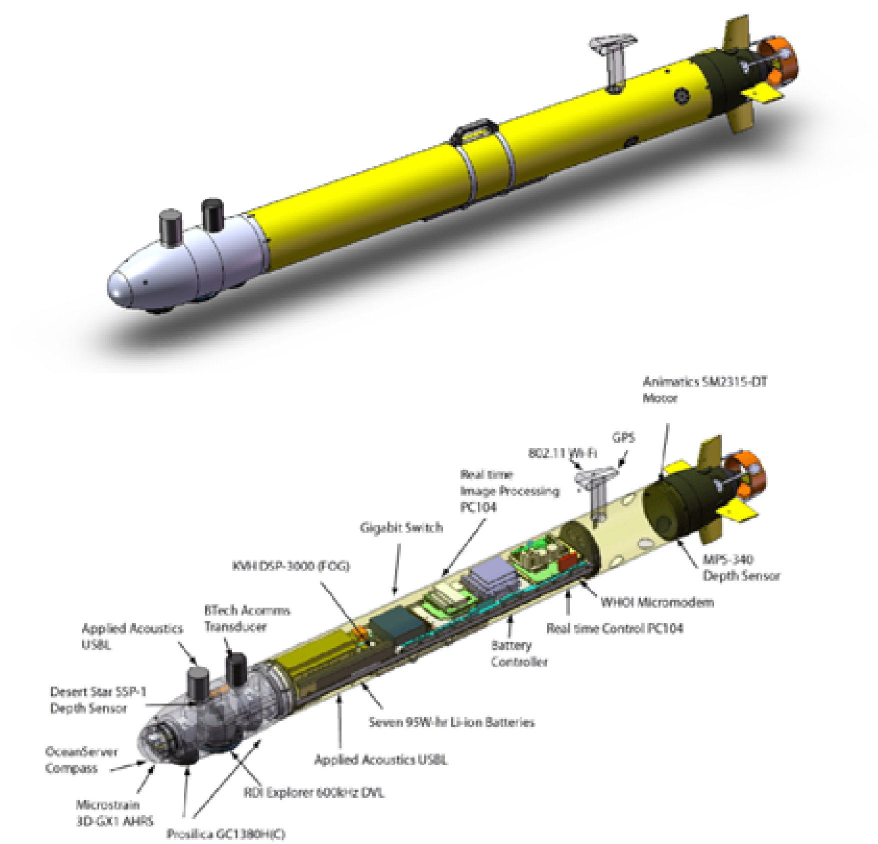

selected as a testbed development platform because of its ability to be transported in a personal vehicle and launched by a single user. The vehicles, as shipped, are rated to a depth of 100 m, have a maximum survey speed of approximately 2 m/s (4 knots), and weigh approximately 30 kg allowing for transport by two people (Anderson and Crowell, 2005).

Because the commercial-off-the-shelf Iver2 vehicle does not come equipped with camera or DVL sensing, sensor upgrades were required to enable the stock vehicle to perform SLAM and coordinated multi-AUV missions. PeRL upgraded the vehicles with additional navigation and perception sensors (detailed in Figure 6b and Table 1), including 12-bit stereo down-looking Prosilica cameras, a Teledyne RD Instruments (RDI) 600 kHz Explorer DVL, a KVH Industries, Inc. (KVH) single-axis fiber-optic gyroscope (FOG), a Microstrain 3DM-GX1 attitude-heading-reference sensor, a Desert Star SSP-1 digital pressure sensor, and a WHOI Micro-modem for inter-vehicle communication. For illumination, we contracted the custom design and fabrication of a LED array by Farr and Hammar Engineering Services, LLC. To accommodate the additional sensor payload, a new Delrin nose cone was designed and fabricated. An additional 32-bit embedded PC104 CPU hardware was added for data-logging, real-time control, and *in situ* real-time SLAM algorithm testing and validation. Details of the design modification are discussed herein.

## Mechanical/Electrical Design and Integration

The design goals during the integration phase of vehicle development consisted of minimizing the hydrodynamic drag, maintaining the neutral buoyancy, and maximizing the sensor payload capacity within the pressure hull. These requirements were achieved

**TABLE 1**

Integrated sensors on the PeRL vehicles.

| Iver2 Instruments | Variable | Update Rate | Precision | Range | Drift |
|---|---|---|---|---|---|
| Ocean-Server OS5000 Compass | Attitude | 0.01-40 Hz | 1-3° (Hdg), 2° (Roll/Pitch) | 360° | – |
| Measurement Specialties Pressure Sensor MSP-340 | Depth | 0.01-40 Hz | <1% of FS† | 0-20.4 atm | – |
| Imagenex Sidescan Sonar (Dual Freq.) | Sonar image | 330 or 800 kHz | – | 15-120 m | – |
| USGlobalSat EM-406a GPS | XYZ position | 1 Hz | 5-10 m | – | – |
| **New Instruments** | | | | | |
| Prosilica GC1380H(C) Camera (down-looking stereo-pair) | Gray/color image | 0.1-20 fps | 1360 × 1024 pixels 12-bit depth | – | – |
| Strobed LED Array‡ | Illumination | 0.1-4 fps | – | 2-4 m altitude | – |
| Teledyne RDI 600 kHz Explorer DVL | Body velocity | 7 Hz | 1.2-6 cm/s (at 1 m/s) | 0.7-65 m | – |
| KVH DSP-3000 1-Axis FOG | Yaw rate | 100 Hz | 1-6° /h | ±375°/s | 4°/h/√Hz |
| Desert-Star SSP-1 300PSIG Digital Pressure Transducer | Depth | 0.0625-4 Hz | 0.2% of FS† | 0-20.4 atm | – |
| Applied Acoustics USBL | XYZ position | 1-10 Hz | ±0.1 m (Slant Range) | 1000 m | – |
| OWTT* Nav (Modem + PPS) | Slant range | Varies | 18.75 cm (at 1500 m/s) | Varies | <1.5 m/14 h |
| •WHOI Micro-modem | Communication | Varies | – | Varies | – |
| •Seascan SISMTB v4 PPS Clock | Time | 1 Hz | 1 μs | – | <1 ms/14 h |
| Microstrain 3DM-GX1 AHRS | Attitude | 1-100Hz | 2° (Hdg), 2° (Roll/Pitch) | 360° | – |
| | Angular rate | 1-100 Hz | 3.5°/s | ±300°/s | 210°/h/√Hz |

†Full scale.
‡In development.
*One-way travel time.

through the use of lightweight materials such as acrylonitrile butadiene styrene (ABS), Delrin, and aluminum, and through careful center of buoyancy and center of mass computations. The entire vehicle was modeled using SolidWorks solid modeling software, and the extensive use of these computer-aided design (CAD) models provided optimal arrangements of internal components prior to actual installation (Figure 7).

The addition of a redesigned SLAM nose cone and sensor payload shifted both the original center of buoyancy and center of gravity. New positions were estimated using the CAD models and refined during ballast tests at the UMich Marine Hydrodynamics Laboratory (MHL). The vehicle is ballasted to achieve approximately 0.11 kg (0.25 lbs) of reserve buoyancy for emergency situations when the vehicle must surface without power. Vehicle trim is set neutral to achieve passive stability and to optimize both diving and surfacing operations.

The interior component arrangement within the main body took into account mass, geometry, heat dissipation, and electrical interference considerations when determining the spatial layout and arrangement of sensors, computing, and electronics in the main tube. Because of the high density of sensors and other devices in the pressure housing, the components with the highest heat radiation, such as computers and DC-DC converters, were placed in direct contact with the aluminum chassis to allow better heat dissipation. Also, sensors that are prone to electrical noise from surrounding electronics were spatially separated in the layout (e.g., the Micro-Electro-Mechanical Systems (MEMS) Microstrain 3DM-GX1 is located in the nose cone tip, the furthest point from the motor and battery pack influence).

Electrically, the vehicle is powered by a 665 Wh Li-ion battery pack made up of seven 95 Wh laptop batteries. This battery pack is managed by an Ocean-Server Intelligent Battery and Power System module. The additional sensors and PC104 computing added by PeRL draw less than 40 W total. This load is in addition to the original 12 W nominal vehicle hotel load and 110 W propulsion load of the stock Iver2, which results in a combined maximum total power draw of approximately 162 W (this assumes full hotel load and the motor at full power). The estimated run time at full load is 4.1 h; however, taking into account a more realistic assessment of propulsion load for photo transect survey conditions, the continuous run time will be closer to 5.2+ h at a 2 knot (i.e., 75 W propulsion) survey speed.

**FIGURE 7**

Mechanical layout.

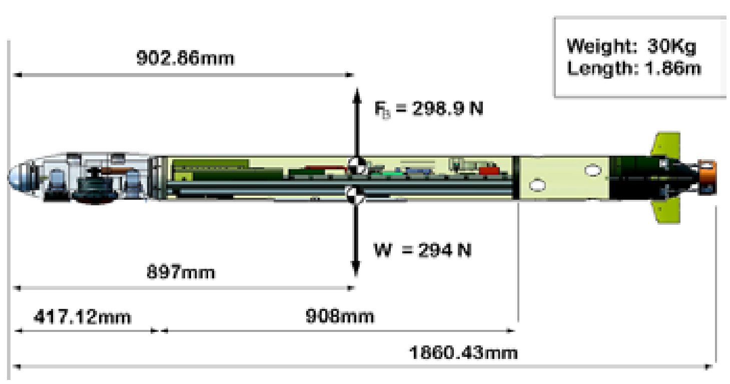


## SLAM Nose Cone

In order to support the real-time visual SLAM objectives of PeRL, a down-looking stereo-vision system was added to the Iver2 vehicles. A dual camera arrangement was chosen because it provides greater flexibility for visual SLAM research. For example, using a stereo-rig allows for the measurement of metrical scale information during pairwise image registration and, thereby, can be used to improve odometry estimation by observing velocity scale error in DVL bottom-track measurements. Additionally, the dual camera arrangement can be used to run one of the cameras in a low-resolution mode suitable for real-time image processing (e.g., VGA or lower), whereas the second camera can be run at its native 1.6 megapixel resolution for offline processing. At depth, illumination will come from a LED array mounted at the aft of the vehicle. The array will provide optimal illumination over a 2-4 m imaging altitude at up to 4 fps strobe rate with a camera-to-light separation distance of approximately 1.25 m.

To accommodate the two-camera vision system and the DVL transducer, a new nose cone was designed and fabricated. The UMich custom-designed nose cone (Figure 8) was fabricated from Acetron GP (Delrin) because of the material's high tensile strength, scratch resistance, fatigue endurance, low friction, and low water absorption. Threaded inserts are installed in the nose cone to prevent stripped threads, and stainless fasteners with a polytetrafluoroethene paste (to prevent corrosion issues) are used in all locations.

**FIGURE 8**

(top) Exploded and transparent view of PeRL's redesigned nose cone. (bottom) The fabricated nose cone as installed.

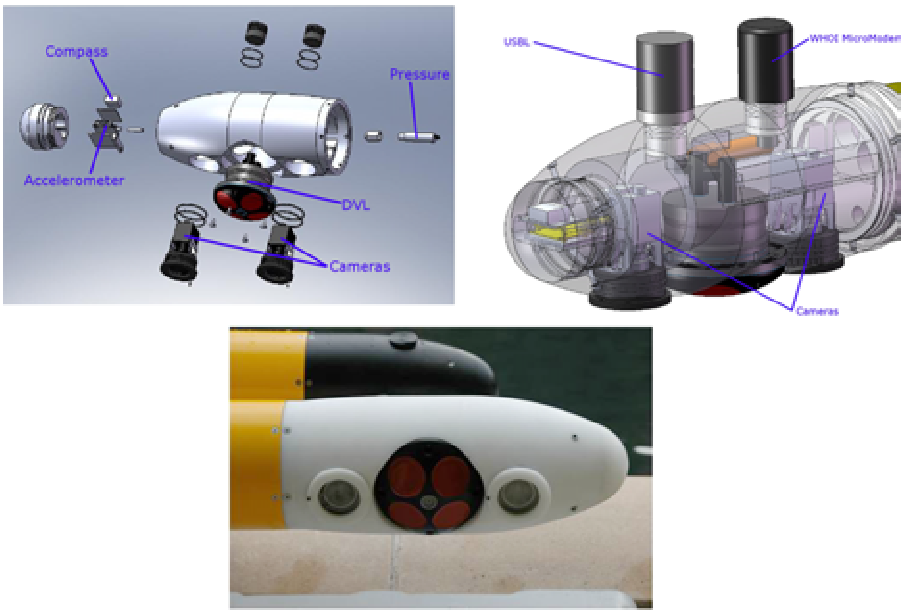


The designed working depth of the nose cone is 100 m (to match the full rating of the Iver2). Calculations were performed according to the ASME Section VIII Boiler and Pressure Vessel Code to verify the wall thickness in each of the nose cone sections. A minimum factor of safety of at least 2.64 was attained for all sections of the nose cone. Pressure tests, conducted at Woods Hole Oceanographic Institution, demonstrated the structural integrity of the nose cone to 240 m water depth. Three short duration tests of 12 min each were made to 24.5 atm (240 m salt water equivalent), and one long duration test of 5 h was made to 24.5 atm.

The Teledyne RDI 600 kHz Explorer DVL is integrated into the nose cone using fasteners to attach the DVL head to threaded inserts in the nose cone material. The limited internal cavity space of the Iver2 nose precludes the use of RDI's recommended clamp attachment method. Instead, self-sealing fasteners are used to eliminate a fluid path through the mounting holes of the DVL to the interior of the nose cone. The associated DVL electronics module is mounted in the main chassis of the vehicle just behind the forward bulkhead. The electronics module and transducer head are connected by RDI's recommended shielded twisted-pair cabling to reduce stray electromagnetic field effects.

Two nose cone plugs were designed for camera integration. These plugs include a sapphire window and two mounting brackets each (Figure 8). The synthetic sapphire window was custom designed and fabricated by the Optarius Company of the U.K. Sapphire was chosen because of its high scratch resistance and superior tensile strength to that of plastic or glass materials. The mounting brackets were designed in CAD and printed in ABS plastic using a Dimension Fused Deposition Modeling (FDM) Elite rapid prototype machine. Static face and edge o-ring seals prevent water ingress through the plug around the sapphire window.

A Desert Star SSP-1 pressure transducer is mounted to an internal face of the nose cone and is exposed to the ambient environment through a 1/8 in. shaft drilled perpendicular to the nose cone wall to reduce the flow noise influence on the sensor. The Microstrain 3DM-GX1 is integrated into the nose cone tip by mounting the Ocean-Server OS5000 compass on top of the 3DM-GX1 and milling a cavity in the tip to allow additional vertical clearance. All o-rings installed in the nose cone are of Buna-N (acrylonitrile-butadiene) material and are lightly lubricated with Dow Corning #4 prior to installation.

## Mission Planning and Control

The stock Iver2 control computer is a 500 MHz AMD Geode CPU running Windows XP Embedded for the operating system. Ocean-Server provides a Graphical User Interface (GUI) mission planning module called VectorMap (Figure 11) and a vehicle control software called Underwater Vehicle Control (UVC). The VectorMap mission planning software allows the user to graphically layout a mission trajectory over a geo-registered image or nautical navigation chart and to specify parameters such a depth, speed, goal radius, timeout, and other attributes for each waypoint. The output of VectorMap is an ASCII waypoint file that the UVC loads and executes within a Proportional-Integral-Derivative (PID) control framework (Leveille, 2007). Additionally, the UVC supports a backseat driver Application Programming Interface (API) interface for user-level control from a host client. This API supports two control primitives: (1) a high-level control interface where the host specifies the reference heading, speed, and depth set points, and (2) a low-level control interface where the host specifies servo commands for the thruster and control surfaces.

The modified PeRL vehicle uses a Digital-Logic ADL945 1.2 GHz Core-Duo PC104 for backseat control and data logging. The ADL945 runs less than 10 W in power consumption, has Gigabit Ethernet for interfacing with the Prosilica GigE cameras, and runs 32-bit Ubuntu Linux. The host stack records data from the cameras and navigation sensors, performs online state estimation, and directs the real-time control of the Iver2 via the backseat driver API. For ease of software development and modularity, we have adopted a multi-process software paradigm that uses the open-source LCM inter-process communication library developed by the Massachusetts Institute of Technology (MIT) Defense Advanced Research Projects Agency (DARPA) Urban Grand Challenge team (Leonard et al., 2008; LCM, 2009).

## Missions and Testing

Current missions and testing conducted by PeRL include testing at the UMich MHL tow tank, automated visual ship-hull inspection (conducted at AUV Fest 2008), field testing at the UMich Biological Station, and archaeological surveys of shipwrecks in the Thunder Bay National Marine Sanctuary.

### UMich Marine Hydrodynamics Laboratory

The UMich MHL provides a controlled experimental environment for testing real-time underwater visual SLAM algorithms. The freshwater physical model basin measures 110 m × 6.7 m × 3.0 m (Figure 9) and can achieve prescribed vehicle motions via the electronically controlled tank carriage. Trajectory ground-truth is obtained from the encoder measured carriage position and will be used to validate real-time visual SLAM pose estimates derived from registering the imagery of the tank floor. For ease of real-time algorithm development, we can attach a wet-mateable wired Ethernet connection to a vehicle bulkhead so that imagery and sensor data can be streamed live to a topside desktop computer. This allows for greater flexibility in real-time software development, visualization, and debugging. The use of the test facility has been beneficial for early development and testing of our Iver2 hardware and real-time underwater visual SLAM algorithms.

### AUV Fest 2008

The Iver2 serves as a testbed for real-time visual autonomous port and hull inspection algorithm research at UMich. We use the Iver2 as a proxy for visual hull inspection by developing and testing our algorithms to navigate over the seafloor (because the underlying visual navigation algorithm is fundamentally the same in the two scenarios). This allows us to use the Iver2 to validate the accuracy of our visually augmented navigation method, and to test and implement our real-time algorithms on the type of embedded system hardware typically found on AUVs.

Meanwhile, to test our VAN algorithms in a real hull-inspection scenario, PeRL collaborated with MIT and Bluefin Robotics at AUV Fest 2008 to put one of our camera systems on the Hovering Autonomous Underwater Vehicle (HAUV) (Vaganay et al., 2005). In this experiment, we collected imagery of the hull of the USS Saratoga—a decommissioned U.S. aircraft carrier stationed at Newport, Rhode Island (Figure 10a). PeRL packaged and mounted a calibrated Prosilica GC1380HC camera (the same camera system used in the Iver2 SLAM nose cone) and a flash strobe light system on the HAUV hull inspection vehicle. Boustrophedon survey imagery was collected by the HAUV of the hull of the USS Saratoga. The

**FIGURE 9**

Vehicle testing at MHL tow tank.

**FIGURE 10**

Hull inspection results from AUV Fest 2008. (a) Depiction of the AUV Fest 2008 experimental setup. (b) The camera-derived pose constraints are shown as red and green links. Each vertex represents a node in the pose-graph enclosed by its 3σ covariance uncertainty ellipsoid. Because of the change of the visual feature richness along the hull, the uncertainty ellipsoid inflates when the vehicle is not able to build enough pose constraints but then deflates once VAN creates camera constraints with previous tracklines. Three small figure insets depict the typical feature richness for different regions of the hull. (c) Triangulated 3-D points are fitted to obtain a smooth surface reconstruction and then texture mapped to create a 3-D photomosaic. The six white dots are targets that were manually placed on the hull and used to verify the utility of the visual hull inspection algorithm.

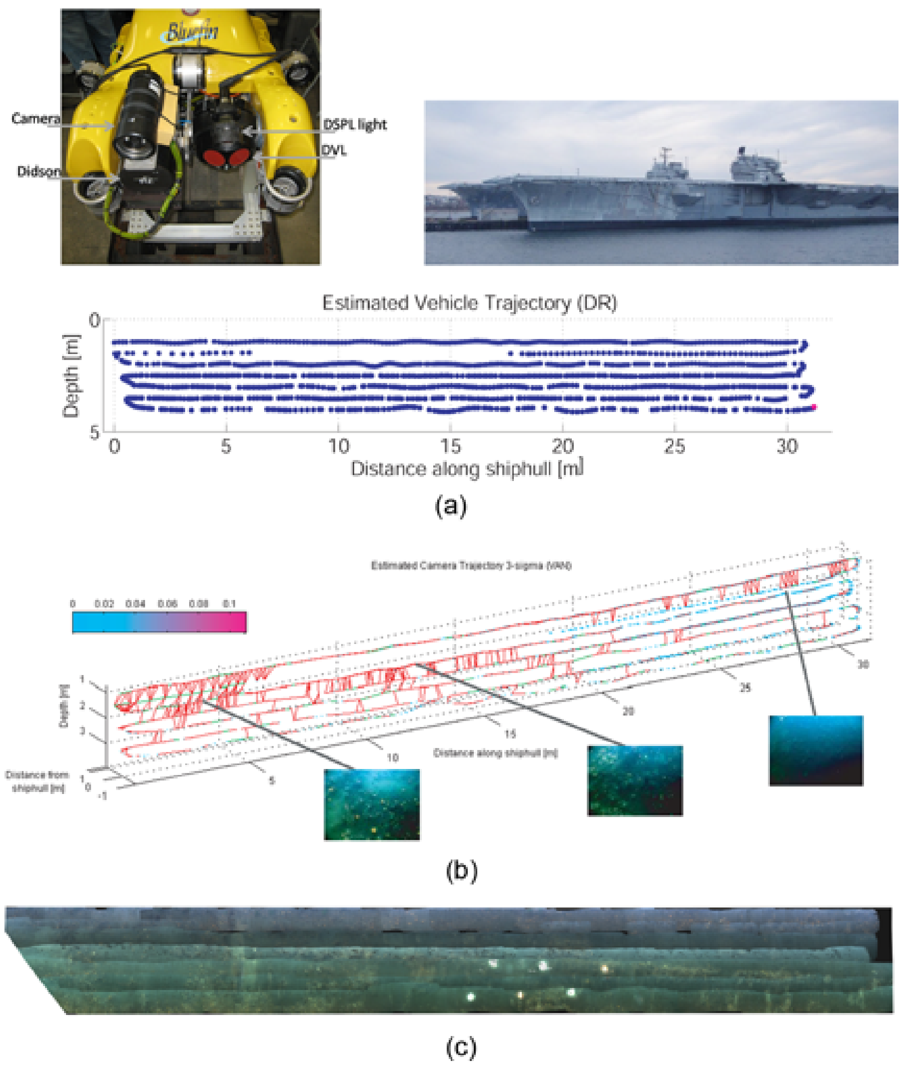


HAUV is equipped with a 1200 kHz DVL, a FOG, and a depth sensor, all of which are comparable to the sensor suite integrated into PeRL's Iver2 testbed.

Preliminary results for visual hull-relative navigation are shown in Figure 10 (Kim and Eustice, 2009). Here, we see a pose-graph of the camera constraints generated through pairwise registration of overlapping imagery. These constraints are fused with navigation data in an extended information filter framework to provide a bounded error precision navigation estimate anywhere along the hull. Each node in the network corresponds to a digital-still image taken along the hull (over 1300 images in all). Note the discrete dropout of imagery along the second leg in the region of 5 m to 20 m along the hull axis. Because of a logging error, we did not record any imagery during this time; however, this gap in the visual data record actually highlights the utility of our hull-referenced visual navigation approach. Because we are able to pairwise register views of the hull taken from different times and locations, the camera-based navigation algorithm is able to "close-the-loop" and register itself to earlier imagery from the first leg of the survey—thereby resetting any incurred DVL navigation error during the data dropout period. It is precisely this hull-referenced navigation capability that allows the AUV to navigate *in situ* along the hull without the need for deploying any external aiding (e.g., acoustic-beacon transponders).

## UMich Biological Station

Field trials were held on Douglas Lake at the UMich Biological Station (UMBS) in Pellston, Michigan, during July 2008. Four days of on-water testing demonstrated maneuverability, vehicle speed, dead-reckon navigation, wireless Ethernet communication, sidescan sonar functionality, digital compass, and manual surface joystick operation modes as summarized in Table 2.

Launch and recovery were conducted from shore, dock, and from a pontoon boat. A full sidescan sonar survey of the southeastern bay at Douglas Lake was run from the UMBS docks (Figure 11). After completion of the mission, the vehicle was manually driven under joy-stick con-

## TABLE 2

Results of testing stock Iver2 at UMBS.

| Attribute | Performance |
|---|---|
| Maneuverability | 1.5 m altitude bottom following |
| | 25 cm depth band control |
| | 4.5 m turning radius |
| Speed | 0.5-1.5 m/s |
| DR navigation accuracy *(DR = prop counts + compass u/w; GPS when on surface)* | 10% distance traveled |
| 802.11g Wi-Fi | 100 m range (on surface) |

trol from a portable wireless station back to the dock for recovery. This onshore launch and recovery capability facilitates the ease of experimental field testing with the Iver2.

### Thunder Bay National Marine Sanctuary

In August 2008, PeRL collaborated with the National Oceanic and Atmospheric Administration (NOAA) Thunder Bay National Marine Sanctuary (TBNMS) researchers to map unexplored areas outside the Sanctuary's current boundaries (Figure 12a). Established in 2000, the TBNMS protects

## FIGURE 11

VectorMap mission-planning interface for the Iver2. The depicted tracklines are for a sidescan sonar survey of a portion of Douglas Lake. Launch and recovery of the Iver2 were performed from a dock on shore.

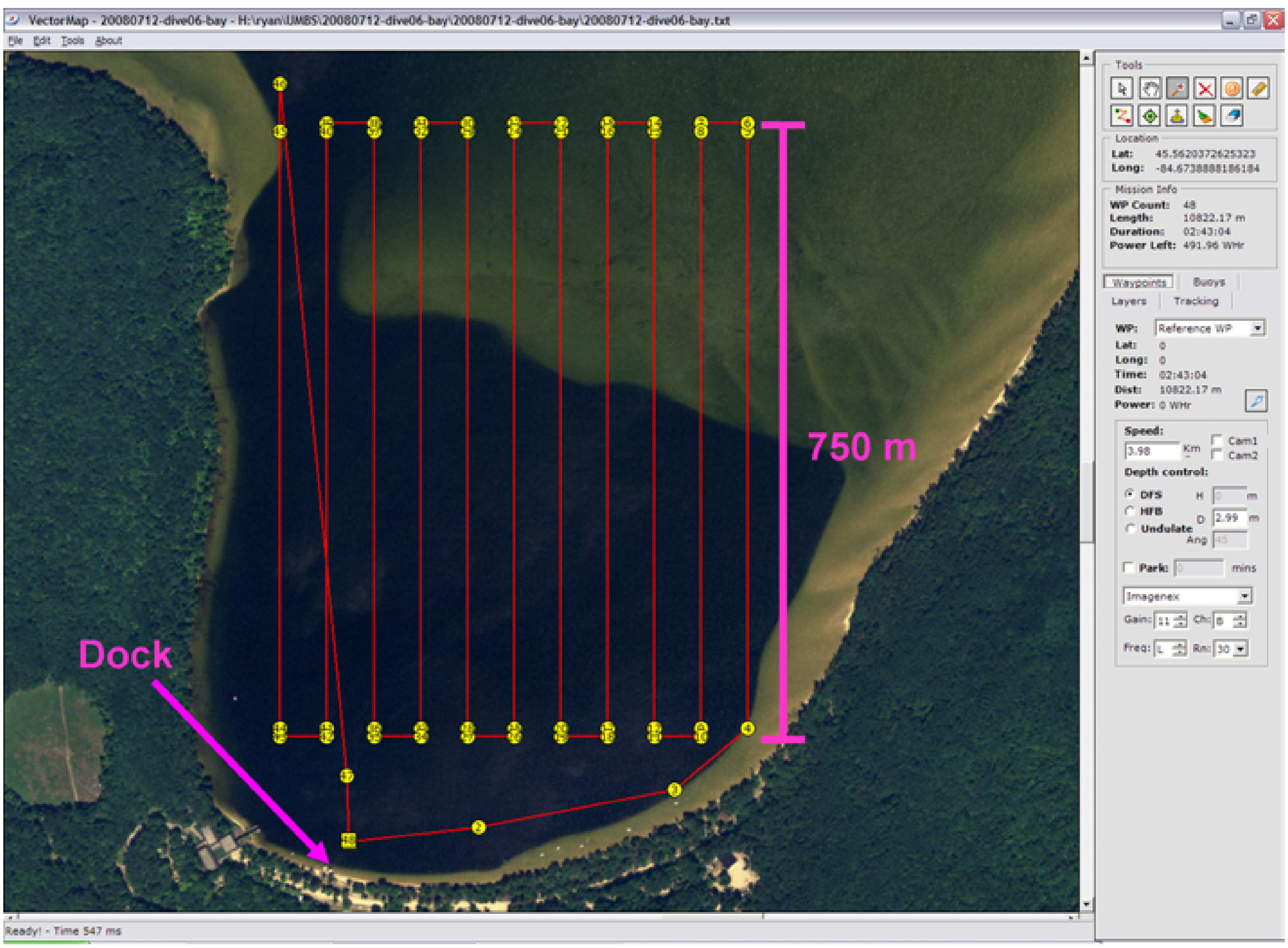

## FIGURE 12

Sidescan sonar mapping results from the 2008 summer field season in TBNMS. (a) Thunder Bay National Marine Sanctuary facility. (b) A large area search was conducted first to locate the target wreck indicated in the white box (survey tracklines are shown in green). A second finer-scale survey was then conducted to map the target at higher resolution (tracklines overlaid in gray). (c) Target imagery found using 330 kHz sonar. (d) Detailed target imagery using 800 kHz sonar.

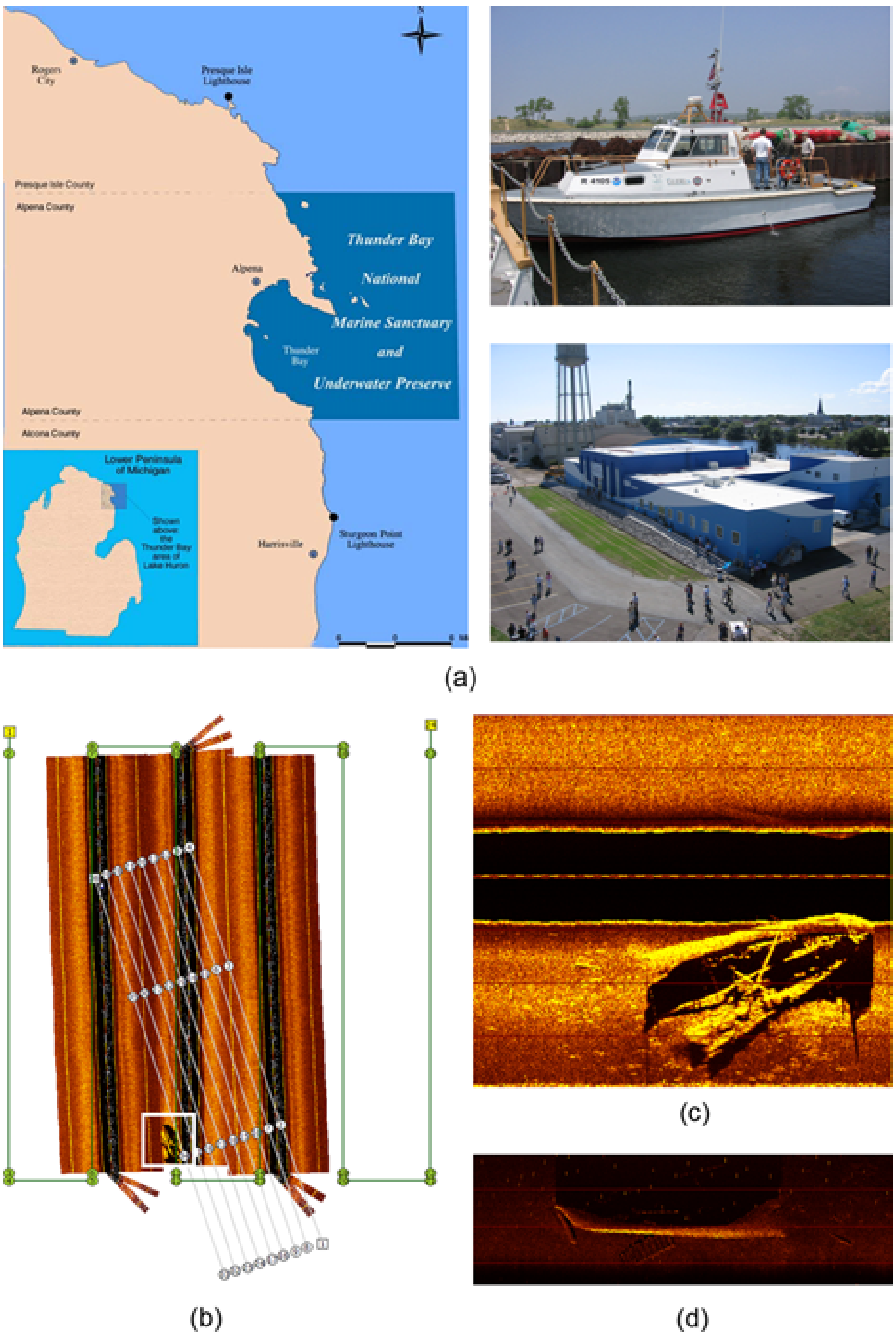


one of the nation's most historically significant collections of shipwrecks. Located in the northeast corner of Michigan's Lower Peninsula, the 448 mi$^2$ sanctuary contains 40 known historic shipwrecks. Archival research indicates that over 100 sites await discovery within and just beyond the sanctuary's current boundaries. This fact, coupled with strong public support and the occurrence of dozens of known shipwrecks, provides the rationale for the sanctuary's desire to expand from 448 mi$^2$ to 3,662 mi$^2$ (an eightfold increase). To date, however, a comprehensive remote sensing survey has not been conducted in the potential expansion area. Moreover, significant portions of the existing sanctuary have not been explored.

PeRL is engaged in a 5-year collaboration effort with TBNMS to use the Sanctuary as a real-world engineering testbed for our AUV algorithms research. TBNMS provides in-kind support of ship time and facilities and in return receives SLAM-derived archaeological data products ranging from 3-D photomosaics of shipwrecks to sidescan sonar maps of the Sanctuary seafloor. In addition, PeRL is engaged in public outreach efforts in collaboration with TBNMS to educate the general public in the use and technology of underwater robotics. In development is an AUV technology display in their state-of-the-art Great Lakes Maritime Heritage Center, (a 20,000 ft$^2$ building featuring a 100-seat theater, 9,000 ft$^2$ of exhibit space, and distance learning capabilities), which will consist of an Iver2 AUV hull, a multimedia kiosk, and maps and data products derived from PeRL's field testing in the Sanctuary.

This past August, as part of an NOAA Ocean Exploration grant, PeRL fielded one of its two Iver2 AUVs to collect sidescan sonar imagery in unmapped regions of the Sanctuary seafloor. Figure 12 shows survey tracklines and sonar imagery collected of a newly found wreck outside of the Sanctuary's boundaries in approximately 50 m of water depth.

## Conclusion

This paper provided an overview of PeRL's AUV algorithms research and testbed development at UMich. To summarize, PeRL's main research thrusts are in the areas of (1) real-time visual SLAM, (2) cooperative multi-vehicle navigation, and (3) perception-driven control. Toward that goal, we reported the modifications involved in preparing two commercial Ocean-Server AUV systems for SLAM research at UMich. PeRL upgraded the vehicles with additional navigation and perceptual sensors, including 12-bit stereo down-looking Prosilica cameras, a Teledyne RDI 600 kHz Explorer DVL for 3-axis bottom-lock velocity measurements, a KVH single-axis FOG for yaw rate, and a WHOI Micro-modem for communication, along with other sensor packages. To accommodate the additional sensor payload, a new Delrin nose cone was designed and fabricated. An additional 32-bit embedded CPU hardware was added for data-logging, real-time control, and *in situ* real-time SLAM algorithm testing and validation. Our field testing and collaboration with the TBNMS will provide a validation of the proposed navigation methodologies in a real-world engineering setting, whereas a new museum exhibit on underwater robotics at their visitor center will disseminate the findings and results of this research to the general public.

## Acknowledgments

This work is supported in part through grants from the National Science Foundation (Award #IIS 0746455), the Office of Naval Research (Award #N00014-07-1-0791), and an NOAA Ocean Exploration grant (Award #WC133C08SE4089).

## References

**Anderson**, B., Crowell, J. 2005. Workhorse AUV—A cost-sensible new autonomous underwater vehicle for surveys/soundings, search & rescue, and research. In Proc. of the IEEE/MTS OCEANS Conference and Exhibition. pp. 1228-1233. Washington, D.C.: IEEE.

**Bailey**, T., Durrant-Whyte, H. 2006. Simultaneous localization and mapping (SLAM): Part II. IEEE Robot. Autom. Mag. 13(3): 108-117.

**Ballard**, R.D. (ed). 2008. Archaeological Oceanography. Princeton, New Jersey: Princeton University Press. 296 pp.

**Bourgault**, F., Furukawa, T., Durrant-Whyte, H. 2004. Decentralized Bayesian negotiation for cooperative search. In Proc. of the IEEE/RSJ International Conference on Intelligent Robots and Systems. pp. 2681-2686. Sendai, Japan: IEEE.

**Durrant-Whyte**, H., Bailey, T. 2006. Simultaneous localization and mapping: Part I. IEEE Robot. Autom. Mag. 13(2):99-110.

**Eustice**, R.M. 2008. Toward real-time visually augmented navigation for autonomous search and inspection of ship hulls and port facilities. In: International Symposium on Technology and the Mine Problem. Monterey, CA: Mine Warfare Association (MINWARA).

**Eustice**, R.M., Singh, H., Leonard, J.J. 2006a. Exactly sparse delayed-state filters for view-based SLAM. IEEE Trans. Robot. 22(6):1100-1114.

**Eustice**, R.M., Singh, H., Leonard, J.J., Walter, M.R. 2006b. Visually mapping the RMS Titanic: Conservative covariance estimates for SLAM information filters. Int. J. Rob. Res. 25(12):1223-1242.

**Eustice**, R.M., Whitcomb, L.L., Singh, H., Grund, M. 2006c. Recent advances in synchronous-clock one-way-travel-time acoustic navigation. In Proc. of the IEEE/MTS OCEANS Conference and Exhibition. pp. 1-6. Boston, MA: IEEE.

**Eustice**, R.M., Whitcomb, L.L., Singh, H., Grund, M. 2007. Experimental results in synchronous-clock one-way-travel-time acoustic navigation for autonomous underwater vehicles. In Proc. of the IEEE/RSJ International Conference on Intelligent Robots and Systems. pp. 4257-4264. Rome, Italy: IEEE.

**Eustice**, R.M., Pizarro, O., Singh, H. 2008. Visually augmented navigation for autonomous underwater vehicles. IEEE J. Oceanic Eng. 33(2):103-122.

**Fleischer**, S. 2000. Bounded-error vision-based navigation of autonomous underwater vehicles. PhD thesis, Stanford University.

**Foley**, B., DellaPorta, K., Sakellariou, D., Bingham, B., Camilli, R., Eustice, R., Evagelistis, D., Ferrini, V., Hansson, M., Katsaros, K., Kourkoumelis, D., Mallios, A., Micha, P., Mindell, D., Roman, C., Singh, H., Switzer, D., Theodoulou, T. 2009. New methods for underwater archaeology: The 2005 Chios ancient shipwreck survey. J. Hesperia. In press.

**Freitag**, L., Grund, M., Singh, S., Partan, J., Koski, P., Ball, K. 2005a. The WHOI micro-modem: an acoustic communications and navigation system for multiple platforms. In Proc. of the IEEE/MTS OCEANS Conference and Exhibition. pp. 1086-1092. Washington, D.C: IEEE.

**Freitag**, L., Grund, M., Partan, J., Ball, K., Singh, S., Koski, P. 2005b. Multi-band acoustic modem for the communications and navigation aid AUV. In Proc. of the IEEE/MTS OCEANS Conference and Exhibition. pp. 1080-1085. Washington, D.C.: IEEE.

**Hunt**, M., Marquet, W., Moller, D., Peal, K., Smith, W., Spindel, R. 1974. An acoustic navigation system. Woods Hole Oceanographic Institution Technical Report WHOI-74-6.

**Kim**, A., Eustice, R.M. 2009. Pose-graph visual SLAM with geometric model selection for autonomous underwater ship hull inspection. In: IEEE/RSJ International Conference on Intelligent Robots and Systems. Submitted for publication.

**Kinsey**, J.C., Eustice, R.M., Whitcomb, L.L. 2006. Underwater vehicle navigation: Recent advances and new challenges. In Proc. of the IFAC Conference on Maneuvering and Control of Marine Craft. Lisbon, Portugal: International Federation of Automatic Control (IFAC).

**LCM**. 2009. Lightweight Communications and Marshalling. http://code.google.com/p/lcm/ (Accessed April 15, 2009).

**Leonard**, J., How, J., Teller, S., Berger, M., Campbell, S., Fiore, G., Fletcher, L., Frazzoli, E., Huang, A., Karaman, S., Koch, O., Kuwata, Y., Moore, D., Olson, E., Peters, S., Teo, J., Truax, R., Walter, M., Barrett, D., Epstein, A., Maheloni, K., Moyer, K., Jones, T., Buckley, R., Antone, M., Galejs, R., Krishnamurthy, S., Williams, J. 2008. A perception-driven autonomous urban vehicle. J. Field Robot. 25(10):727-774.

**Leveille**, E.A. 2007. Analysis, redesign and verification of the Iver2 autonomous underwater vehicle motion controller. Masters thesis, University of Massachusetts Dartmouth.

**Milne**, P. 1983. Underwater acoustic positioning systems. Houston: Gulf Publishing Company. 284 pp.

**Neira**, J., Tardos, J. 2001. Data association in stochastic mapping using the joint compatibility test. IEEE Trans. Robot. Autom. 17(6):890-897.

**Newman**, P.M., Leonard, J.J. 2003. Pure range-only sub-sea SLAM. In Proc. of the IEEE International Conference on Robotics and Automation. pp. 1921-1926. Taipei, Taiwan: IEEE.

**Olson**, E., Leonard, J.J., Teller, S. 2006. Robust range-only beacon localization. IEEE J. Oceanic Eng. 31(4):949-958.

**Ong**, L.L, Upcroft, B., Bailey, T., Ridley, M., Sukkarieh, S., Durrant-Whyte, H. 2006. A decentralised particle filtering algorithm for multi-target tracking across multiple flight vehicles. In Proc. of the IEEE/RSJ International Conference on Intelligent Robots and Systems. pp. 4539-4544. Beijing, China: IEEE.

**Partan**, J., Kurose, J., Levine, B. N. 2006. A survey of practical issues in underwater networks. In: Proc. of the ACM International Workshop on Underwater Networks. pp. 17-24. New York: ACM Press.

**Rekleitis**, I., Dudek, G., Milios, E. 2003. Probabilistic cooperative localization and mapping in practice. In Proc. of the IEEE International Conference on Robotics and Automation. pp. 1907-1912. Taipei, Taiwan: IEEE.

**Ridley**, M., Nettleton, E., Sukkarieh, S., Durrant-Whyte, H. 2002. Tracking in decentralised air-ground sensing networks. In Proc. of the IEEE International Conference on Information Fusion. pp. 616-623. Annapolis, Maryland: IEEE.

**Roman**, C., Singh, H. 2005. Improved vehicle based multibeam bathymetry using submaps and SLAM. In Proc. of the IEEE/RSJ International Conference on Intelligent Robots and Systems. pp. 2422-2429. Edmonton, Alberta, Canada: IEEE.

**Smith**, S., Kronen, D. 1997. Experimental results of an inexpensive short baseline acoustic positioning system for AUV navigation. In Proc. of the IEEE/MTS OCEANS Conference and Exhibition. pp. 714-720. Halifax, Nova Scotia, Canada: IEEE.

**Stewart**, W. 1991. Remote-sensing issues for intelligent underwater systems. In Proc. of the IEEE Conference on Computer Vision and Pattern Recognition. pp. 230-235. Maui, HI, USA: IEEE.

**Vaganay**, J., Elkins, M., Willcox, S., Hover, F., Damus, R., Desset, S., Morash, J., Polidoro, V. 2005. Ship hull inspection by hull-relative navigation and control. In Proc. of the IEEE/MTS OCEANS Conference and Exhibition. pp. 761-766. Washington, D.C.: IEEE.

**Walter**, M.R., Leonard, J.J. 2004. An experimental investigation of cooperative SLAM. In Proc. of the IFAC/EURON Symposium on Intelligent Autonomous Vehicles. Lisbon, Portugal: International Federation of Automatic Control (IFAC).

**Williams**, S.B., Dissanayake, G., Durrant-Whyte, H. 2002. Towards multi-vehicle simultaneous localisation and mapping. In Proc. of the IEEE International Conference on Robotics and Automation. pp. 2743-2748. Washington, D.C.: IEEE.